First-principles studies for CO and O_2 on gold nanocluster

Yao-Ping Xie and Xin-Gao Gong[a)]
Department of Physics, Surface Physics Laboratory, and MOE Key Laboratory of Computational Physical Sciences, Fudan University, Shanghai 200433, China

(Received 1 March 2010; accepted 31 May 2010; published online 22 June 2010)

First-principles calculations are performed to study the interaction of gold nanocluster Au_{55} with small molecules CO and O_2. We find that the adsorption energy of CO on Au_{55} is among 0.5–0.7 eV at different sites and $[CO+O_2]$ can be coadsorbed on Au_{55}. Comparisons between Au_{55} and Au_{32} show that the adsorption energy not only depends on the size of the cluster but also on the geometry of the cluster. Similar with smaller cluster (Au_8 and Au_{32}), the energy difference between $[CO+O_2]$ and $[CO_2+O]$ on Au_{55} is much larger than that in the free gas. Our calculations indicate that the nanocluster Au_{55} can enhance the reaction process, $CO+O_2 \rightarrow CO_2+O$, in which the reaction barrier is only about half electron volts. © *2010 American Institute of Physics*.
[doi:10.1063/1.3455714]

I. INTRODUCTION

The properties of nanoscale material are usually very different from those of the corresponding bulk material. One typical example is catalytic property of nanosize gold particles. Gold had been known as one of the least reactive metals in the bulk phase and hence has been regarded as relatively less important in catalysis for long time.[1] Since the pioneering work of Haruta *et al.*,[2,3] many investigations[4–15] showed that many nanogold systems and nanogold dispersed as fine nanoparticles on metal oxide surfaces facilitate a wide range of oxidation reactions, such as the CO and NO oxidations. The mechanism of the oxidation reaction catalyzed by nanogold attracts much research interests.

For gaining fundamental insights into the CO oxidation on nanogold, intensive studies had been devoted to chemical properties of small gold clusters. Calculations of CO adsorption on $Au_n(n=2-6)$ and O_2 adsorption on $Au_n(n=2-8)$ showed a size-dependent reactivity of gold cluster.[16–18] Both experimental and theoretical studies on Au_2^- ions revealed the detailed reaction mechanism of the catalytic gas phase oxidation of CO, and a key metastable intermediate with a mass of $Au_2CO_3^-$ was observed.[19] An investigation of Au_{10} cluster which mimics the shape of a flat nanoparticle showed that low coordinations are the key factors of catalytic properties.[20] The activity of the tetrahedral Au_{20} cluster was well studied, and its effects of charging and impurity had been revealed.[21] Calculations of two different structures of Au_{32} showed that the cagelike Au_{32} has a higher chemical inertness than the amorphous Au_{32} with respect to the interaction with small molecules CO and O_2.[22] Furthermore, the charge effect of cluster and coadsorption of $[CO+O_2]$ on clusters also obtained detailed investigations.[23–27] Cooperative adsorption of CO and O_2 on small gold clusters was also found experimentally.[26,27] It is worth to mention that recent studies show that coadsorption of O_2 and C_2H_4 on small gold clusters can also occur,[28,29] which is important to understanding the mechanism of catalytic oxidation. However, most of clusters which are used to study the interactions of the clusters with CO and O_2 have the number of atoms no more than 32. Since the most reactive nanoparticles are found in the 2–4 nm range in CO oxidation, studies on larger cluster are certainly necessary and important to understand the CO oxidation. Recently, the structure of medium-sized clusters 55–64 atoms (1.1–1.3 nm in diameter) had been investigated.[30–36] These clusters with diameter larger than 1 nm belong to a critical size regime connecting small gold clusters to gold nanoparticles. For a fundamental understanding of gold nanocluster catalysis property, in this paper we choose Au_{55} as an example to investigate interaction of nanocluster with CO and O_2.

II. THEORETICAL METHODS

The present calculations are based on the density functional theory[37,38] and plane-wave basis set[39,40] with generalized gradient approximation,[41,42] which are implemented in the VASP code.[43] Since PW91 appears to describe the adsorption of O_2 on some transition metals more accurately,[44,45] and PW91 was used in many previous studies of interaction CO and O_2 with gold,[22,23,45–47] in the present study we take PW91 for the exchange-correlation potentials. The interaction between core and valence electrons is described with the projector augmented wave potential.[48,49] The structures of the clusters and the corresponding complexes are optimized by the conjugate gradient method.[50] A simple cubic supercell with a lattice constant of 20, 25, and 30 Å is adopted for Au_8, Au_{32}, and Au_{55}, respectively, which is large enough to neglect the interaction between the cluster and its periodic images. Due to the large super cell, only Γ point in the Brillouin zone is used for *K*-space sampling. The structures of clusters are first optimized in coincidence with the previous theoretical studies,[30,51] then the small molecules, i.e., CO, O_2, or O atom, are added on for the calculation of complexes. The cutoff energies for the plane-wave basis set are

a)Electronic mail: xggong@fudan.edu.cn.

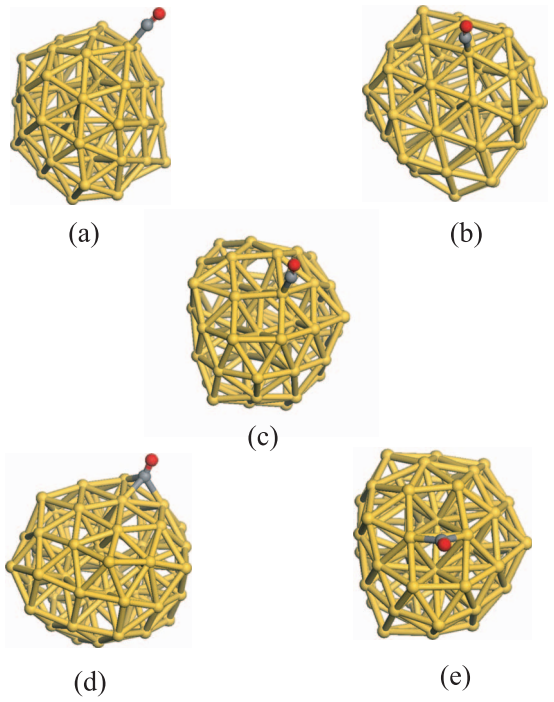

FIG. 1. Relaxed structures of CO on cluster Au_{55} at different sites. Gray balls denote C atom, red balls denote O atom, yellow balls denote Au atom. (a) Five-coordinated surface site, (b) six-coordinated surface site, (c) five-coordinated surface site near defect area, (d) triangle center site, and (e) bridge site near defect area.

all 400 eV for adsorbates, bare, and adsorbates adsorbed gold clusters.

III. RESULTS

Both previous calculations and experiments show that nanocluster Au_{55} possesses an amorphouslike structure.[32–35] It is shown that the cluster Au_{55} has a nonicosahedral disordered structure with strong surface contractions analogous to bulk surface reconstructions, which can be seen in Fig. 1. In the surface of the optimized Au_{55} structure, some atoms are five-coordinated and the others are six-coordinated. In addition, the square defect can easily be recognized at the surface of Au_{55} structure.

In order to investigate the adsorption property of CO on Au_{55} cluster, the structure of Au_{55}–CO complexes are optimized. Due to the complicate surface of Au_{55}, five typical adsorption sites are selected to study the behavior CO on Au_{55} cluster. The structures of these complexes are shown in Fig. 1 and the corresponding adsorption energies are listed in Table I. Figures 1(a) and 1(b) show the structure in which CO is absorbed on the top of five- and six-coordinated sites. The CO adsorption energies are 0.71 and 0.50 eV for five-site and six-coordinated sites, respectively. It indicates that CO on Au_{55} is more favorable on the lower five-coordinate site, which is similar with CO absorbed on Au_{32} cluster.[22] Figure 1(c) shows the structure which CO is absorbed on the top of five-coordinated site near the square defect. The adsorption energy is 0.52 eV for defect site which is 0.19 eV lower than that of five-coordinate site within no defect area. It is shown that not only the coordinate but the defect also affects the adsorption energy. Besides adsorption on top site,

TABLE I. The properties for the interaction of CO with cluster Au_{55}: CO adsorption energy (E_{ad}), C–O bond length (r(C–O)), and Au–C bond length (r(Au–C)). The positions are shown in Fig. 1.

Position	E_{ad} (eV)	r(C–O) (Å)	r(Au–C) (Å)
(a) Five-coordinated	0.71	1.15	1.98
(b) Six-coordinated	0.50	1.15	2.02
(c) Five-coordinated[a]	0.52	1.15	2.00
(d) Triangle center	0.70	1.18	2.10
(e) Bridge	0.67	1.18	2.17

[a]Within defect area.

the adsorption on the triangle center site of the surface and bridge site on Au_{55} can also be calculated. Figure 1(d) shows the structure which CO is absorbed on triangle center site. Figure 1(e) shows the structure in which CO is absorbed on bridge site of two atoms of the square defect. The adsorption energy of CO on triangle site and bridge site are 0.70 and 0.67 eV.

The above results show that CO can be absorbed on Au_{55} with significant adsorption energy. Meanwhile, the adsorption energies are among 1.0–1.1 eV for amorphous metastable Au_{32},[22] and the adsorption energies are 0.84 and 0.40 eV for five- and six-coordinate sites on high symmetry cagelike Au_{32}, respectively. These data suggest that the CO adsorption energies are strongly size-dependent. Furthermore, CO adsorption energy on the six-coordinate of amorphous Au_{55} (0.50 eV) is even larger than that of smaller cagelike stable Au_{32} (0.40 eV), which indicates that the amorphous structure plays an important role for the enhancement of the reactivity of Au_{55}.

Next, we discuss the structural properties of these Au_{55}–CO complexes. It is found that the structure of Au_{55} does not change too much after adsorbing CO. For structures of CO absorbed on top of the Au_{55}, all the CO bonds in above three structures increase to 1.15 Å, and the Au–C bonds are 1.98, 2.00, and 2.02 Å, in comparison of the bond length 1.14 Å of free CO. In the last two complexes as shown in Fig. 1, CO is bound by three or two gold atoms simultaneously, and the C–O bond increases to 1.18 Å. Previous study showed that CO bonds on Au_{32} were stretched to 1.15 Å which is equal to the CO^- bond, accompanying charge transfer from gold atom to CO. In the view of the Dewar–Chatt–Duncanson mode,[52] the bonding of Au–C involves the charge transfer from the Au to the antibonding π^* orbit of CO (donation) and backdonation to the Au from the CO bonding σ orbit. The occupied-antibonding π^* orbit of CO results to the elongation of C–O bond length. Similar to the case of Au_{32}, the bond of CO on Au_{55} is also stretched. This suggests that the charge should be transferred from gold atom to CO resulting chemical adsorption.

The charge density distribution can qualitatively reveal the charge transfer from Au_{55} to CO. We plot charge distribution of highest occupied state [highest occupied molecular orbital (HOMO)] of three Au_{55}–CO systems in Fig. 2. Figure 2(a) is the case for the CO weakly bonded to Au_{55} at six-coordinated site, in which the distance of Au and C atom is 3.2 Å. Figures 2(b) and 2(c) are for the cases of CO ab-

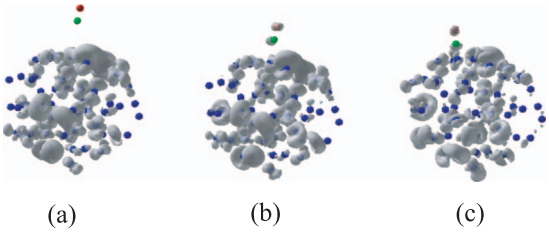

FIG. 2. The charge distribution of highest occupied state (HOMO) of clusters Au_{55}–CO system. The plots show equal density surface. (a) Free CO on six-coordinated surface site, (b) CO absorbed on six-coordinated surface site, and (c) CO absorbed on triangle center site.

sorbed on six-coordinated and triangle center sites, respectively. Comparing Fig. 2(a) with Figs. 2(b) and 2(c), one can see that some HOMO charges are distributed around CO indicating partial charge transfer to CO.

Our calculations show that the adsorption energies of O_2 are 0.08 and 0.10 eV on six- and five-coordinate sites of Au_{55}, respectively, indicating physical adsorption. We turn to investigate the coadsorption of O_2 and CO on Au_{55}. Several typical examples of coadsorption on different sites on Au_{55} are calculated and results are listed in Table II. As shown in Fig. 3(a), an O_2 molecular is added on an adjacent six-coordinate site near CO. In this complex, the adsorption energy of $[CO+O_2]$ is 0.83 eV. Compared to the sum of the adsorption energy of O_2 and CO, 0.58 eV (0.50 eV +0.08 eV) (Tables I and II), the increase of the adsorption energy for the coadsorption of $[CO+O_2]$ amounts to 0.25 eV so the presence of a preadsorbed CO on the neighboring Au atom notably enhances the binding of O_2 to the Au_{55}. In the case of coadsorption of $[CO+O_2]$ involving strong-binding

TABLE II. The properties for the coadsorption of CO and O_2 on cluster Au_{55}: adsorption energy (E_{ad}) of various adsorbates on the cluster, increase of adsorption energy (ΔE_{ad}), and the shortest distance (d) between the adsorbate and the cluster.

Adsorbate	E_{ad} (eV)	ΔE_{ad} (eV)	d (Å)
	O_2: six-coordinated		
O_2	0.08		2.76
	O_2: five-coordinated		
O_2	0.10		2.33
	CO, O_2: six-coordinated (neighboring)		
O_2	0.08		2.76
$CO+O_2$	0.83	0.25	1.99(CO)/2.89(O_2)
	CO: six-coordinated, O_2: five-coordinated (neighboring)		
O_2	0.05		2.56
$CO+O_2$	0.87	0.11	1.98(CO)/2.56(O_2)
	CO: five-coordinated, O_2: six-coordinated (neighboring)		
O_2	−0.05		2.14
$CO+O_2$	0.57	0.12	1.97(CO)/2.14(O_2)
	CO, O_2: six-coordinated (separated)		
O_2	0.08		2.76
$CO+O_2$	0.82	0.24	1.98(CO)/3.23(O_2)

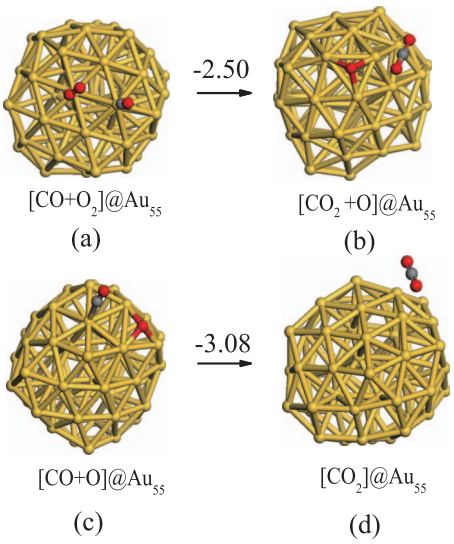

FIG. 3. Relaxed structures of $CO+O_2$, CO_2+O, O_2, and atomic O on cluster Au_{55}. The total energy (in eV) changes between neighboring structures are shown, and the negative denotes the total energy of right structures lower than left one.

sites, the O_2 is bonded much closer to the cluster, we still find that coadsorption can lead to an energy gain more than 0.1 eV. The enhancement effect also exists, when the O_2 is added on the site far from the site that CO absorbed on. These results indicate that coadsorption can clearly enhance the binding for $[CO+O_2]$ on the Au cluster. The possible reason could be due to the charged Au cluster arising from a partial charge transfer to preadsorbed CO.

Two reaction mechanisms[45,53–56] for the CO oxidation on nanogold are known: (1) the Langmuir–Hinshelwood (LH) mechanism, in which the coadsorbed CO and O_2 molecules react to form a peroxo-type complex intermediate, i.e., $CO+O_2 \rightarrow CO_2+O$, and (2) the Eley–Rideal (ER) mechanism, in which the gas phase CO molecules directly react with activated O_2, i.e., $CO+O \rightarrow CO_2$. For the ER mechanism, the presence of the atomic O is a necessary condition. The very small adsorption energy of O_2 indicates that atomic O cannot be provided by direct dissociation of O_2. The ER process only can occur after LH process so the LH mechanism becomes critical for CO oxidation on Au_{55}. For understanding of the role of Au_{55} in the CO oxidation, we have calculated the total energy of free CO, O, O_2, CO, and various Au_{55}–C–O complexes. Coadsorptions of $CO+O_2$, CO_2+O, $CO+O$, and CO_2 on Au_{55} are considered for Au_{55}–C–O, while corresponding adsorption energies are listed in Table III. We first compare the total energy of reactant $[CO+O_2]$

TABLE III. The properties for the interaction of CO, O, O_2, and CO_2 with cluster Au_{55}: adsorption energy (E_{ad}) of various adsorbates on the cluster and the shortest distance (d) between the adsorbate and the cluster.

Adsorbate	E_{ad} (eV)	d (Å)
$CO+O_2$	0.83	1.99(CO)/2.89(O_2)
CO_2+O	3.27	3.06(CO_2)/2.13(O)
$CO+O$	3.65	2.02(CO)/2.17(O)
CO_2	0.01	2.85

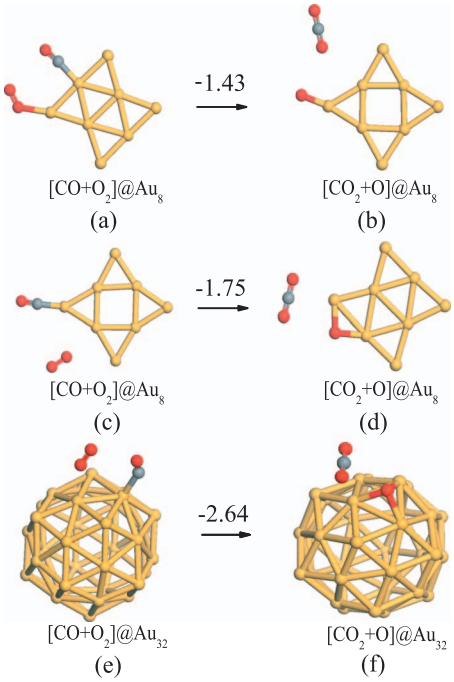

FIG. 4. Relaxed structures of $CO+O_2$, CO_2+O, O_2, and atomic O on cluster Au_8 and Au_{32}. The total energy (in eV) changes between neighboring structures are shown, and the negative denotes the total energy of right structures lower than left one.

and product $[CO_2+O]$ in LH mechanism process for free gas, and it is found the total energy of the later is only slightly lower than the former by 0.09 eV. Then, we compare the total energy of corresponding complex structure of $Au_{55}-C-O$. The total energy of $[CO_2+O]$ at Au_{55} [see Fig. 3(b)] is lower than that of complex $[CO+O_2]$ at Au_{55} structure [Fig. 3(a)] by 2.50 eV. The presence of Au_{55} brings new Au–C bond and Au–O bond, resulting in a larger difference of total energy between $[CO_2+O]$ at Au_{55} and $[CO+O_2]$ at Au_{55}. Such energy difference is significantly larger than that of free gas phase, which indicates that the $CO+O_2$ is more easy to convert into CO_2+O on cluster Au_{55}, i.e., the gold cluster makes the LH mechanism more favorable. Obviously, the LH process on the Au_{55} surface is exothermic.

Then, we compare the total energies of $[CO+O]$ and CO_2 both on the cluster and in the free gas phase. The total energy of the later is lower than the former by 6.72 eV. However, the total energy of $[CO+O]$ at Au_{55} [see Fig. 3(d)] is only lower than that of complex $[CO_2]$ at Au_{55} structure [Fig. 3(c)] by 3.08 eV. It suggests that the $[CO+O]$ can be converted into CO_2 on Au_{55} with ER mechanism. However, the energy difference for $[CO+O]$, $[CO_2]$ on Au_{55} is smaller than that in the gas phase. So comparable to the gas phase, one can find that the ER process is weakened by Au_{55}.

For comparisons of Au_{55} with smaller cluster, we study some Au_8-C-O and $Au_{32}-C-O$ complexes. Coadsorptions of $[CO+O_2]$ and $[CO_2+O]$ are considered for $Au_{32}-C-O$ and Au_8-C-O, respectively. Figure 4 displays the stable structures of Au_8-C-O and $Au_{32}-C-O$ complexes. The adsorption energies and structural properties, i.e., bond length,

TABLE IV. The properties for the interaction of CO, O, O_2, and CO_2 with cluster Au_8, Au_{32}: adsorption energy (E_{ad}) of various adsorbates on the cluster and the shortest distance (d) between the adsorbate and the cluster.

Adsorbate	E_{ad} (eV)	d (Å)
Au_8 (CO: four-coordinated, O_2: two-coordinated)		
$CO+O_2$	1.02	2.01(CO)/2.24(O_2)
CO_2+O	2.53	3.64(CO_2)/1.91(O)
Au_8 (CO: two-coordinated, O_2: four-coordinated)		
$CO+O_2$	1.23	1.95(CO)/2.92(O_2)
CO_2+O	3.07	3.01(CO_2)/1.96(O)
Au_{32} (CO, O_2: six-coordinated)		
$CO+O_2$	0.30	2.08(CO)/3.14(O_2)
CO_2+O	3.03	3.15(CO_2)/2.11(O)

are listed in Table IV. It is shown that the $[CO+O_2]$ can also be absorbed on Au_8 and Au_{32}. The cluster Au_8 has lower coordinate, resulting in a relatively larger adsorption energy 1.02 (1.23) eV than that of Au_{55}. In addition, we can see in Figs. 4(a) and 4(d) that the adsorption of CO or O can induce structure transition of Au_8. This had been also observed and discussed by previous work.[29,57] The structure of Au_{32} with high symmetry has a perfect surface, resulting in relatively smaller adsorption energy of 0.30 eV. Examination of total energy of Au–C–O complexes is preformed. It is found that Au_8 and Au_{32} also make the $[CO_2+O]$ more stable, which indicates that these clusters make the LH process of CO oxidation easier. The energy difference of $[CO+O_2]$ at Au_8 and $[CO_2+O]$ at Au_8 is 1.43 (1.75) eV. The energy difference of $[CO+O_2]$ at Au_{32} and $[CO_2+O]$ at Au_{32} is 2.64 eV. From the above discussion, the Au_8, Au_{32}, and Au_{55} have similar effect for CO oxidation. All these structures can coabsorb the $[CO+O_2]$, and make the LH process much easier

Finally, kinetic factors are also important to understand the process of the CO oxidation.[58] We use the nudged elastic band (NEB) method to compute the reaction barrier of LH process on Au_{55}, comparing that of Au_8 and Au_{32}. The initial and final states in NEB calculations are Figs. 3(a) and 3(b)

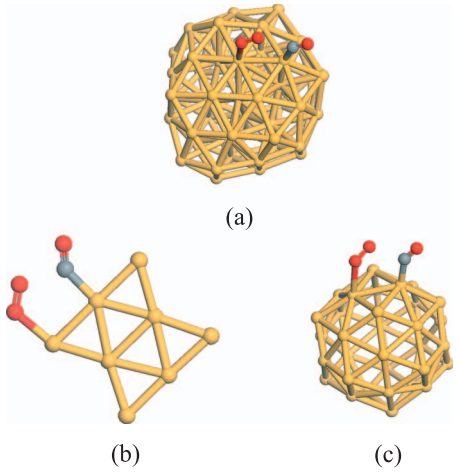

FIG. 5. Structures of the adsorbates on the Au_{55} at transition state for $CO+O_2 \rightarrow CO_2+O$ (LH process).

TABLE V. The structural property for the transition states of Au_8, Au_{32}, and Au_{55} for $CO+O_2 \rightarrow CO_2+O$: bond length of molecular and the shortest distance between the adsorbate and the cluster.

d (Å)	Au_8	Au_{32}	Au_{55}
$d_{(Au-O)}$	2.25	2.80	2.86
$d_{(O1-O2)}$	1.28	1.26	1.26
$d_{(O2-C)}$	2.18	2.34	2.66
$d_{(C-O)}$	1.16	1.15	1.15
$d_{(C-Au)}$	2.04	2.07	2.00

for Au_{55}, Figs. 4(a) and 4(b) for Au_8,[59] and Figs. 4(e) and 4(f) for Au_{32}, respectively. The structures of the adsorbates on the clusters at transition states are shown in Fig. 5, and the corresponding structural parameters are listed in Table V. It is shown, in all the transition states, that the bonds of O_2 are stretched, when two molecules come closer. The reaction barriers of Au_8, Au_{32}, and Au_{55} are 0.45, 0.42, and 0.56, respectively. The results of the barrier are only about 0.5 eV, thus CO oxidation can easily occur.[54,55] Interestingly, recent investigation shows that a crown high symmetry Ih-Au at Cu_{12} at Au_{42} cluster is also potentially capable of catalyzing the CO oxidation.[60] The reaction barrier of LH process of this crown cluster is 0.61 eV, which is slightly higher than that of amorphous Au_{55} with same size.

IV. CONCLUSION

In conclusion, we have carried out the first-principles calculations to investigate the interactions of nanocluster Au_{55} with CO and O_2. We find that CO can be adsorbed on Au_{55} at different sites, but the adsorption energy of O_2 is very small. However, CO and O_2 can be coadsorbed on Au_{55}. Moreover, it is also found that the adsorption properties of gold cluster are not only sensitive to the size of cluster but are also dependent on the cluster geometry. Although both the LH and ER processes for the CO oxidation are possible on Au_{55}, the cluster Au_{55} can make LH($CO_2+O_2 \rightarrow CO_2+O$) process more favorable from view of thermodynamic driving. Since the adsorption of O_2 on Au_{55} is weak, the ER processes can only start after LH process. Finally, we have searched the minimum-energy pathway for the LH process on Au_{55}.

In the present work, we have investigated the interaction of CO and O_2 molecules with nanocluster Au_{55}. However, some interesting problems are beyond the scope of the present work, such as electronic interaction of the gold nanocluster with the support. We wish the present study can shield light for the understanding more complex reactions in gold clusters, such as alcohol oxidation, selective epoxidation, etc., and contribute to comprehensive understanding of unusual catalytic properties of nanogold.

ACKNOWLEDGMENTS

The authors thank Professor Z. Zhang for critical discussions. This work was supported by the National Science Foundation of China, the special funds for major state basic research, the Shanghai municipal, and the MOE support. The computation is performed at Fudan supercomputer center.

[1] B. Hammer and J. K. Nøskov, Nature (London) **376**, 238 (1995).
[2] M. Haruta, T. Kobayashi, H. Sano, and N. Yamada, Chem. Lett. **2**, 405 (1987).
[3] M. Haruta, N. Yamada, T. Kobayashi, and S. J. Iijima, J. Catal. **115**, 301 (1989).
[4] M. Valden, X. Lai, and D. W. Goodman, Science **281**, 1647 (1998).
[5] M. Haruta, S. Tsubota, T. Kobayashi, H. Kageyama, M. J. Genet, and B. Delmon, J. Catal. **144**, 175 (1993).
[6] M. Okumura, S. Nakamura, S. Tsubota, T. Azuma, and M. Haruta, Catal. Lett. **51**, 53 (1998).
[7] S. J. Lee and A. Gravriilidis, J. Catal. **206**, 305 (2002).
[8] J. D. Grunwaldt and H. Teunissen, Europe Patent No. EP 1,209,121 (2002).
[9] F. Boccuzzi, A. Chiorino, M. Manzoli, and M. Haruta, J. Catal. **202**, 256 (2001).
[10] R. J. H. Grisel and B. E. Nieuwenhuys, J. Catal. **199**, 48 (2001).
[11] M. M. Schubert, S. Hackenberg, A. C. van Veen, M. Muhler, V. Plzak, and R. J. Behm, J. Catal. **197**, 113 (2001).
[12] W. An, Y. Pei, and X. C. Zeng, Nano Lett. **8**, 195 (2008).
[13] B. Hvolbæk, T. V. W. Janssens, B. S. Clausen, H. Falsig, C. H. Christensen, and J. K. Nørskov, Nanotoday **2**, 14 (2007).
[14] P. Pyykkö, Chem. Soc. Rev. **37**, 1967 (2008).
[15] R. Coquet, K. L. Howard, and D. J. Willock, Chem. Soc. Rev. **37**, 2046 (2008).
[16] B. Yoon, P. Koskinen, B. Huber, O. Kostko, B. von Issendorff, H. Häkkinen, M. Moseler, and U. Landman, ChemPhysChem **8**, 157 (2007).
[17] B. Yoon H. Ha1kkinen, and U. Landman, J. Phys. Chem. A **107**, 4066 (2003).
[18] X. Wu, L. Senapati, S. K. Nayak, A. Selloni, and M. Hajaligol, J. Chem. Phys. **117**, 4010 (2002).
[19] L. D. Socaciu, J. Hagen, T. M. Bernhardt, L. Wöste, U. Heiz, H. Häkinen, and U. Landman, J. Am. Chem. Soc. **125**, 10437 (2003).
[20] I. N. Remediakis, N. Lopez, and J. K. Nørskov, Appl. Catal., A **291**, 13 (2005).
[21] L. M. Molina and B. Hammer, J. Catal. **233**, 399 (2005).
[22] Y. Wang and X. G. Gong, J. Chem. Phys. **125**, 124703 (2006).
[23] D. W. Yuan and Z. Zeng, J. Chem. Phys. **120**, 6574 (2004).
[24] G. E. Johnson, N. M. Reilly, E. C. Tyo, and A. W. Castleman, J. Phys. Chem. C **112**, 9730 (2008).
[25] B. Yoon H. Hä kkinen, U. Landman, A. S. Wörz, J. Antonietti, S. Abbet, K. Judai, and U. Heiz, Science **307**, 403 (2005).
[26] J. Hagen, L. D. Socaciu, M. Elijazyfer, U. Heiz, T. M. Bernhardt, and L. Woste, Phys. Chem. Chem. Phys. **4**, 1707 (2002).
[27] W. T. Wallace and R. L. Whetten, J. Am. Chem. Soc. **124**, 7499 (2002).
[28] A. Lyalin and T. Taketsugu, J. Phys. Chem. C **113**, 12930 (2009).
[29] A. Lyalin and T. Taketsugu, J. Phys. Chem. C **114**, 2484 (2010).
[30] W. Huang, M. Ji, C. D. Dong, X. Gu, L. M. Wang, X. G. Gong, and L. S. Wang, ACS Nano **2**, 897 (2008).
[31] H. Häkkinen, M. Moseler, O. Kostko, N. Morgner, M. A. Hoffmann, and B. V. Issendorff, Phys. Rev. Lett. **93**, 093401 (2004).
[32] J. P. K. Doye and D. J. Wales, New J. Chem. **22**, 733 (1998).
[33] I. L. Garzón, M. Michaelian, M. R. Beltrán A. Posada- Amarillas, P. Ordejón, E. Artacho, D. Sánchez-Portal, and J. M. Soler, Phys. Rev. Lett. **81**, 1600 (1998).
[34] K. Michaelian, N. Rendon, and I. L. Garzon, Phys. Rev. B **60**, 2000 (1999).
[35] L. Xiao, B. Tollberg, X. K. Hu, and L. C. Wang, J. Chem. Phys. **124**, 114309 (2006).
[36] C. D. Dong and X. G. Gong, J. Chem. Phys. **132**, 104301 (2010).
[37] P. Hohenberg and W. Kohn, Phys. Rev. **136**, B864 (1964); W. Kohn and L. J. Sham, *ibid.* **140**, A1133 (1965).
[38] R. O. Jones and O. Gunnarsson, Rev. Mod. Phys. **61**, 689 (1989).
[39] R. Car and M. Parrinello, Phys. Rev. Lett. **55**, 2471 (1985).
[40] M. C. Payne, M. P. Teter, D. C. Allan, T. A. Arias, and J. D. Joannopoulos, Rev. Mod. Phys. **64**, 1045 (1992).
[41] Y. Wang and J. P. Pedew, Phys. Rev. B **44**, 13298 (1991).
[42] J. P. Perdew, J. A. Chevary, S. H. Vosko, K. A. Jackson, M. R. Pederson, D. J. Singh, and C. Fiolhais, Phys. Rev. B **46**, 6671 (1992).
[43] G. Kresse and J. Furthmüller, Phys. Rev. B **54**, 11169 (1996); Comput. Mater. Sci. **6**, 15 (1996).
[44] B. Hammer, L. B. Hansen, and J. K. Nøskov, Phys. Rev. B **59**, 7413

(1999).
[45] M. Mavrikakis, P. Stoltze, and J. K. Nøskov, Catal. Lett. **64**, 101 (2000).
[46] Y. Xu and M. Mavrikakis, J. Phys. Chem. B **107**, 9298 (2003).
[47] S. A. Varganov, R. M. Olson, M. S. Gordon, and H. Metiu, J. Chem. Phys. **119**, 2531 (2003).
[48] P. E. Blöchl, Phys. Rev. B **50**, 17953 (1994).
[49] G. Kresse and D. Joubert, Phys. Rev. B **59**, 1758 (1999).
[50] M. P. Teter, M. C. Payne, and D. C. Allan, Phys. Rev. B **40**, 12255 (1989).
[51] X. Gu, M. Ji, S. H. Wei, and X. G. Gong, Phys. Rev. B **70**, 205401 (2004).
[52] J. Chatt and L. A. J. Duncanson, J. Chem. Soc. 2939 (1953).
[53] C. Zhang, B. Yoon, and U. Landman, J. Am. Chem. Soc. **129**, 2228 (2007).
[54] N. Lopez and J. K. Nøskov, J. Am. Chem. Soc. **124**, 11262 (2002).
[55] Z. P. Liu, P. Hu, and A. J. Alavi, J. Am. Chem. Soc. **124**, 14770 (2002).
[56] Z. P. Liu, X. Q. Gong, J. Kohanoff, C. Sanchez, and P. Hu, Phys. Rev. Lett. **91**, 266102 (2003).
[57] H. J. Zhai, L. L. Pan, B. Dai, B. Kiran, J. Li, and L. S. Wang, J. Phys. Chem. C **112**, 11920 (2008).
[58] L. K. Ono and B. Roldan Cuenya, J. Phys. Chem. C **112**, 18543 (2008).
[59] In presented NEB calculation, the imputed position of initial state structure is that a CO_2 molecule is physisorbed on the structure of Au_8 like Fig. 4(a) with a chemisorbed atomic O nearby, but structure in Fig. 4(b). The calculation shows that the transition of structure occurs after the break of O–O bond and formation of C–O bond.
[60] Y. Gao, N. Shao, Y. Pei, and X. C. Zeng, Nano Lett. **10**, 1055 (2010).